Joint Optimization of Energy Management and Network Load Balancing in 5G-Enabled Micro-Grids

Sofia Rodríguez-Ramos, Yonas G. Tsegaye

Sofia Rodríguez-Ramos, Institute for Data Science, University of Amsterdam, Science Park 904, 1098 XH Amsterdam, Netherlands;

ABSTRACT In this paper, we focus on the design of energy self-sustainable mobile networks, by enabling intelligent energy management that allows the base stations to mostly operate off-grid by using renewable energies. Many papers are available in the literature on this problem, however, we are approaching this issue from a different angle. In fact, we advocate for future mobile networks with a hierarchical cell structure and powered by energy harvesting hardware. Base stations within the same geographical area are grouped in a micro-grid and operate almost autonomously from the power grid. To achieve this goal, we target the design of optimal traffic and computational load control method with energy sharing within the micro-grid. We solve the optimization problem using a graph-based method and we demonstrate, via software simulations, that a combination of load control plus energy sharing represents a viable and economically convenient solution for enabling energy self-sustainability of mobile networks grouped in micro-grids.

INDEX TERMS Energy harvesting, energy saving, energy sharing, energy storage, green networking, mobile networks, optimization, renewable energy, smart grid, sustainability.

I. INTRODUCTION

to mobile networks and services [4]. From the literature review emerges that the most promising approach to reduce VER the last decade, we have experienced an intense the energy consumption of a mobile network is to enable research effort for green communication networks, spe- sleep modes in some active network elements during periods

Ogrid connected and island mode. Similarly, the European Union recently released the EU Winter Package, aimed at providing guidelines for the next generation of power grids. The main idea is to foster cooperation among local energy communities by providing them with the infrastructure to work in island mode and with market-based retail energy prices.

Recently, the use of sustainable energy for supplying network elements, like base stations (BSs), referred to as eNodeBs in LTE technology, has attracted the research community [8]. This interest is driven by the higher efficiency of mobile equipment and the affordable price of the additional energy harvesting hardware, specially when installed to supply small BSs [9]. Such a solution is proved to be environmentally and economically sustainable not only in rural regions but even in urban environments [10].

Here, we approach the problem from a different angle. In fact, we envision a radio access network (RAN) setup where a hierarchical cell structure is deployed within the same geographical area with BSs of different scale factors, transmission power, computational capabilities and coverage areas [11]. Moreover, thanks to the introduction of the Mobile Edge Computing (MEC) technology [12], BSs can leverage cloud computing capabilities and share part of their computational processes (e.g., baseband processing). Following [13], the federation of BSs together with the distributed energy harvesters and storage systems form a micro-grid, whose operations are coordinated by an energy management system.

In this paper, we elaborate on the intelligent control of the energy harvested and stored from the renewables. In particular, we propose an optimal traffic and computational load control method with energy sharing (LC-ES) among the mobile micro-grid elements, which jointly may enable a greater degree of autonomy from the power grid. The proposed solution has been applied to two different RAN architectures, namely HetNets and MEC-enabled HetNets (MEC-H) [14]. Our optimal method relies on a-priori knowledge of the system variables (i.e., energy harvesting and traffic demand processes). The results provided together with the conclusions drawn may serve as guidelines in the design of self-sustainable mobile networks.

The contributions of the paper are summarized in the list below:

- integration of distributed energy harvesting and storage systems in RANs with heterogeneous BSs deployment in urban environments;

- theoretical formulation of the joint load control and energy sharing optimization problem;
- design of a joint optimal traffic and computational load control plus energy sharing method for two different mobile network architectures, namely HetNets and MEC-H;
- dimensioning of the energy harvesting and storage system and characterization of the network performance;
- energy saving and cost analysis for different energy harvesting and storage design approaches;
- identification of open issues and future research directions for sustainable mobile networking.

The paper is organized as follows. In Section II, we present the state of the art in load control and energy sharing in mobile networks. In Section III, we describe the reference framework. In Section IV we describe the system model. In Section V, we introduce the optimization problem and the methodology used for its solution. Then, in Section VI, we discuss results on the dimensioning of the harvesting and storage system, the optimal SBS configuration policies and the energy shared within the micro-grid. In Section VII, we provide an energy and cost analysis of the two studied architectures. Finally, in Section VIII, we identify open issues and propose future research directions. We draw our conclusions in Section IX.

II. RELATED WORK

In the scientific literature, the proposed approaches to manage BSs supplied by energy harvesters and storage system can be classified into two categories:

1) Energy sharing: BSs are interconnected with electric wires and form a microgrid that enables energy exchange among the BSs.
2) Communication cooperation: BSs cooperate through radio communication mechanisms such as power control, bandwidth control, sleep mode, and traffic offloading and typically are not connected to form a micro-grid. Communication cooperation has been deeply investigated in the last years: especially BS sleep mode and traffic offloading solutions have been studied, as testified by the vivid literature presented in [5]. Alternatively, energy sharing methods among BSs have attracted the interest of the research community more recently.

An architectural solution for the deployment of the microgrid is presented in [15], where an entity named *aggregator* is introduced. The aggregator is in charge of mediating between the grid operator and a group of BSs to redistribute the energy flows. In [16], the authors propose an algorithm that jointly optimizes the transmit power of BSs and the transferred energy to maximize the sum-rate throughput for all the users. This joint communication and energy cooperation problem is proven to be convex. Numerical simulation shows that this approach achieves better performance than no cooperation or cooperation through communication in terms of average sum-rate.

A novel paradigm for sharing is presented in [17], where the concept of the Energy Packet Network (EPN) is introduced. In an EPN, discrete units of energy, termed energy packets, can be exchanged among network elements or acquired from the environment through harvesting hardware. In some approaches [18], the packet takes the form of a pulse of current with fixed voltage and duration. Each energy packet is equipped with an encoded header, containing the information about the destination identity (i.e., its address), which is used to route the energy packet through the EPN. However, the cost of deploying the micro-grid infrastructure that would be required by an EPN can be high. In [19], [20], the use of wireless energy transfer is considered as a means to avoid the installation cost of electric cables. Nevertheless, such technology has a low energy transfer efficiency nowadays, see [21], [22].

Based on our literature review, the definition of joint load control and energy sharing policies is an open field of research, specially in deployments with hierarchical cell structure within the same geographical area and different computational capabilities. The study proposed in this paper aims at filling this gap by providing a joint optimization of sleep mode and computational offloading with energy sharing in a HetNet powered by renewable energy and with MEC capabilities.

III. REFERENCE FRAMEWORK

The next generation of mobile networks will be composed of heterogeneous BSs densely deployed, possibly including different wireless technologies (LTE, New Radio, mmWave, etc.) for both radio access and back/front-haul. A multi-tier architecture is foreseen, where Macro BSs (MBSs) provide baseline coverage and capacity and Small BSs (SBSs) are deployed mainly to enhance the capacity in the hotspots (the so-called HetNets). Densification significantly increases the offered capacity to end-users through frequency reuse. However, it results in a larger number of resources to be managed. MEC architecture jointly with Software-Defined Networking (SDN) and Network Function Virtualization (NFV) paradigms [23] are candidate enablers for automated network management, flexibility and cost reductions. In MEC-H scenario [14], multi-tier MEC servers are co-located at the BSs and have different computational and transmission capabilities (i.e., MBSs are high-power and high-computing nodes). In this work, we are interested in the case that MBSs may support SBSs and enable computational offloading of some of their networking functions. For doing this, a standardized interface, e.g.

Openflow [24], can be used to implement the interactions between the MBSs and SBSs. In this way, SBSs transmission functions are decoupled from proprietary hardware-dependent implementations and may be executed in a different hardware resource of the network. To this respect, 3GPP has defined different functional splits between the distributed and the centralized unit [25], in our case the SBSs and the MBSs, respectively.

In our proposed framework, mobile networks are divided into clusters, each one composed of a MBS and a set of SBSs in its coverage. Each cluster may implement HetNet or MEC-H. In the case of MEC-H architecture, the baseband functions of the SBSs may be opportunistically executed locally or at the MEC server located at the MBS site based on the functional split configurations defined in [25]. The MBS is connected to the power grid, thus assuring a reliable connection for baseline coverage, capacity and processing. The SBSs are powered solely by a photovoltaic (PV) panel plus battery and are deployed for capacity enhancement. Among other harvesting technologies, the solar power is deemed the most appropriate due to the good efficiency of commercial PV panels as well as the wide availability of the solar source for typical installations [26]. Each cluster forms a microgrid and the renewable energy inflow is managed based on a harvest-store-share approach. The power produced by the PV panel is consumed by the SBS and any excess is stored in the battery for a later use. Whenever the battery has reached its maximum capacity, the excess power is shared with the MBS that will use it to reduce the grid energy consumption. The micro-grid is implemented by deploying power lines. Low resistive losses (i.e., the amount of energy lost in the conductor in form of heat) are guaranteed by the short distances between the MBS and the SBSs. When the SBSs have exceeding energy that is not needed by the MBS, that energy is locally dissipated and not injected in the microgrid. In this way, the energy balance in the micro-grid is maintained.

A proper harvesting and storage system design and dimensioning is needed to avoid outage and energy waste. In fact, it may happen that the SBS must be turned off because the PV is not producing enough energy and the battery is empty or that some of the power produced by the PV panel is lost because it cannot be stored nor shared. Consequently, a control architecture is crucial to prolong the network survival. A central control entity named Intelligent Energy Management System (IEMS) is located at the MBS and it is in charge of managing the operative states of the SBSs with the goal of achieving efficient utilization of the harvested energy. In detail, the IEMS opportunistically switches ON/OFF the SBSs in HetNets. Moreover, it decides where to execute the baseband functions of the SBSs in MEC-H deployments. The operational states of the SBSs in both architectures depend on the dynamics of the traffic demands and the energy harvesting arrivals. Therefore, the IEMS is in charge of predicting the evolution of those two processes to prevent SBSs blackout during periods with low renewable energy arrivals and high traffic demands. The Energy Controller (EC) is an entity located at the SBS site that implements the decision taken by the IEMS. The full control architecture is shown in Fig. 1.

IV. SYSTEM MODEL

A. NETWORK MODEL

We consider a two-tier network composed of clusters of one MBS and N SBSs. The system evolves in cycles based on the variation of the traffic demand and the energy arrivals in time. The traffic load experienced at time t by each SBS, generated by the users in their coverage, is defined as $L^t = [L_1^t, L_2^t, \ldots, L_N^t]$. The energy harvested by the SBSs at time t is defined by $H^t = [H_1^t, H_2^t, \ldots, H_N^t]$ and the energy stored by each SBS in its battery at time t is defined by $B^t = [B_1^t, B_2^t, \ldots, B_N^t]$. In particular, the energy stored in the batteries B^{t+1} at the beginning of the next slot is evaluated according to the following formula:

$$B^{t+1} = \min\left(\boldsymbol{B}^t + \boldsymbol{H}^t - \boldsymbol{P}^t\Delta_t, B_{\text{cap}}\right) \quad (1)$$

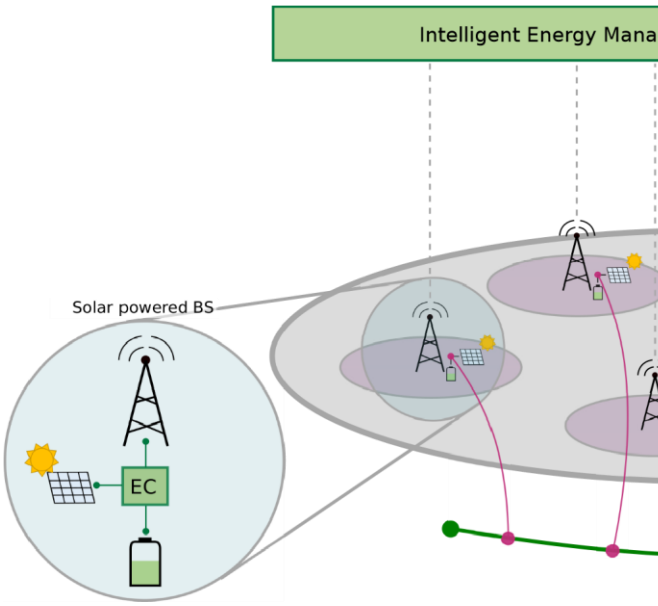

FIGURE 1. Diagram illustrating the reference framework, including the radio access network with r connections. In left-bottom side, a simplified scheme of the solar-powered Base Station is shown.

where $P^t = [P_1^t, P_2^t, \ldots, P_N^t]$ is the power consumed by the BSs at time t, described in Section IV-B, and B_{cap} is the maximum battery capacity. The amount of harvested energy that exceeds the battery capacity is defined as $X^t = [X_1^t, X_2^t, \ldots, X_N^t]$ and it is calculated as:

$$X^{t+1} = \max\left(\boldsymbol{B}^t + \boldsymbol{H}^t - \boldsymbol{P}^t\Delta_t - B_{\text{cap}}, 0\right) \quad (2)$$

The operative state of the SBSs at time t is defined by

$S^t = [S_1^t, S_2^t, \ldots, S_N^t]$. At each cycle, the IEMS decides the optimal configuration of the mobile cluster to serve the traffic demand in that area. The general optimization problem may be formulated as follows:

$$\text{P1:} \min_{\{S^t\}_t, \ldots, K} \sum_{t=1}^{K} f(S^t, t) \quad (3) \quad \text{subject to} \quad B_i^t > B_{\text{th}} \; \forall i.$$

where B_{th} is the battery threshold level and K is the time horizon or the number of times the energy control is applied; $f(S^t,t)$ is the weighted cost function at time step t, which is defined as:

$$f(S^t,t) = w_1 \cdot \mathrm{E_m}(S^t,t) + w_2 \cdot \mathrm{D}(S^t,t) \quad (4)$$

where $\mathrm{E_m}(S^t,t)$ and $\mathrm{D}(S^t,t)$ are respectively the normalized grid energy consumption and the traffic drop rate in the cluster, given the operative modes of the SBSs and the time step t.

The objective is to minimize the energy drained from the grid and avoid system outage. We define system outage as the event to not satisfy the traffic demand due to battery energy depletion or wrong configuration decisions, which may overload the MBS. The grid energy consumption at time t is equivalent to the difference between the MBS energy consumption and the excess energy shared by the SBSs. The normalized grid energy consumption is then computed as:

$$\mathrm{E_m}(S^t, t) = \max\left(\frac{\mathrm{P_m}(S^t, t)\Delta_t - \sum_{i=1}^{N} X_i^t}{\mathrm{P_m^{MAX}}\Delta_t}, 0\right) \quad (5)$$

where $\mathrm{P_m}(S^t,t)$ is the grid power consumption of the MBSs given the operative modes of the SBSs and the time step t, whereas $\mathrm{P^{MAX}_m}$ is the power consumption of the MBS at full load. The traffic drop rate at time t, $\mathrm{D}(S^t,t)$, is the ratio of the total amount of traffic demand that cannot be served by the system in the time step t. Additionally, each battery at the SBSs has to be maintained in the proper State Of Charge (SOC) (i.e, above the battery level threshold B_{th}) to avoid a rapid reduction of its lifetime [27]. Finally, the weights w_1 and w_2 provide flexibility in the cost function to emphasize one part of the cost over the other. They must always be positive and sum to 1, that is, $w_1 \geq 0$, $w_2 \geq 0$, $w_1 + w_2 = 1$.

In the HetNet scenario, each SBS can be switched ON to serve the users in its coverage, or switched OFF to save local energy. In the OFF state, the users in its coverage are handed over the MBS. More in details, the state of a generic SBS i at time t is defined as:

$$S_i^t = \begin{cases} 0 & \text{if the } i\text{-th SBS is OFF} \\ 1 & \text{if the } i\text{-th SBS is ON} \end{cases} \quad (6)$$

In the MEC-H deployment, we target two functional split configuration options based on [25] and listed below:

- PHY-RF split: all the protocols, Physical (PHY) and above layers, are implemented at the MEC server located in the MBS site. Hence, the SBS behaves as a Radio Frequency (RF) transceiver, used only for signal transmission and reception;

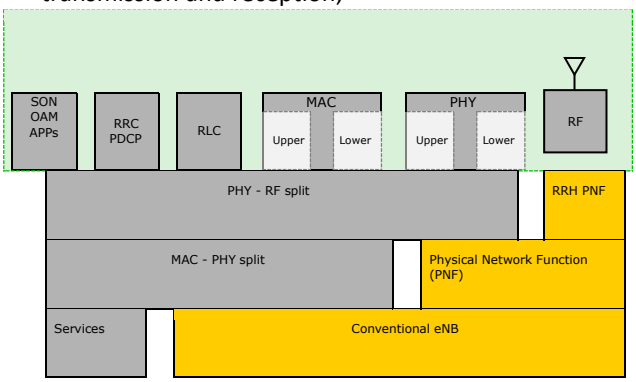

FIGURE 2. The different implementations of the functional split configuration options for a small BS, including Standard PHY-RF and MAC-PHY split. The conventional eNodeB (eNB) configuration is also shown for comparison.

- MAC-PHY split: PHY layer processing takes place at the SBS, in addition to RF functions. Medium Access Control (MAC) and above layer functions are executed by the MEC server at the MBS site.

The diagram in Fig. 2 represents the different implementations of the functional split configuration options compared to the conventional eNodeB architecture. Each operative mode corresponds to different computational load for the SBSs and MBSs, which, in turns, corresponds to different energy consumption models, as will be described in Section IV-B.

It is worth highlighting here that in PHY-RF split, the SBSs are executing only the RF functionalities and the other upper layer functions, including PHY and MAC, are executed at the MBS site. This is similar to a Cloud RAN (CRAN) architecture. Therefore, MEC-H deployment relies on a reconfigurable front-haul since the bandwidth and latency requirements become more stringent when more functions are placed in the centralized unit [28].

In this case, the state of the generic SBS i at time t is defined as:

$$S_i^t = \begin{cases} 0 & \text{if the } i\text{-th SBS is OFF if the } i\text{-th SBS is in} \\ 1 & \text{PHY-RF split mode if the } i\text{-th SBS is in} \\ 2 & \text{MAC-PHY split mode} \end{cases} \quad (7)$$

B. POWER CONSUMPTION MODEL

The power consumption is computed according to the model introduced in [29], which is a general flexible power model of LTE eNodeBs.

The total BS power consumption is given by:

$$P_{BS} = P_{BB} + P_{RF} + P_{PA} + P_{overhead} \quad (8)$$

where P_{BB} is the power consumption due to the baseband processing, P_{RF} is the power consumption due to RF circuitry, P_{PA} is the power consumption by the power amplifier and $P_{overhead}$ is the overhead power consumption (e.g., cooling system).

Baseband power consumption, P_{BB} is given by:

$$P_{BB} = [P_{CPU} + P_{OFDM} + P_{filter} + P_{FD} + P_{FEC}] \quad (9)$$

where P_{CPU} is the idle mode power consumption, P_{OFDM} is the power consumption due to OFDM processes, P_{filter} is the power consumption due to filtering, P_{FD} is the frequency domain processing power consumption and P_{FEC} is the power consumption due to forward error correction (FEC) processes. In accordance with [29], all the terms in (9) are dependent on the number of antennas and bandwidth.
Moreover, P_{FD} and P_{FEC} are the only components that depend on the traffic load.

Considering the MEC-H architecture, when the SBSs are in PHY-RF split mode, their power consumption model does not include the corresponding P_{BB}, since the baseband processing takes place at MBS. Instead, the corresponding P_{BB} term is added to the MBS. On the other hand, in MACPHY split mode, the SBS power consumption includes the baseband power consumption term and is given in (8). In fact, we claim here that the power consumption of a SBS in MAC-PHY split mode is almost equivalent to a conventional eNodeB due to the negligible impact of the MAC and upper layers implementation on the energy budget.

Considering the aforementioned model description, the grid power consumed by the MBS is computed as:

$$P_m = \begin{cases} P_{BS}^{MBS}, & \text{in HetNet} \\ P_{BS}^{MBS} + \sum_{i \in G} P_{BB}^{i}, & \text{in MEC-H} \end{cases} \quad (10)$$

where P_{BS}^{MBS} is the power consumption of the MBS computed as in (8), P_{BB}^{i} is the baseband power consumption of the i-th SBS and G is the set containing the SBSs in PHY-RF split mode.

C. ENERGY HARVESTING AND DEMAND PROFILES

Hourly energy generation traces from a solar source have been obtained for the city of Los Angeles (CA, USA). The solar raw irradiance data have been collected from the National Renewable Energy Laboratory and converted, accounting for a specific solar power technology, into harvested energy traces using the SolarStat tool [30]. For the PV modules, we have considered the commercial Panasonic N235B. These panels have single cell efficiencies as high as 21.1%, which ranks them amongst the most efficient solar modules at the time of writing, delivering about 186 W/m^2.

The energy harvesting traces are generally bell-shaped with a peak around midday, whereas the energy harvested during the night is negligible. Moreover, as discussed in [30], high variability of the harvested energy may occur during the day and this also holds for the summer months. This means that, although the energy inflow pattern can be known to a certain extent, intelligent and adaptive algorithms that make their decisions based on current and past inflow patterns, as well as predictions of future energy arrivals, have to be designed.

For the demand profile, it is commonly accepted and confirmed by measurements that the energy use of base stations is time-correlated and daily periodic. In this article, we use the load profile obtained in [31] for residential urban environment.

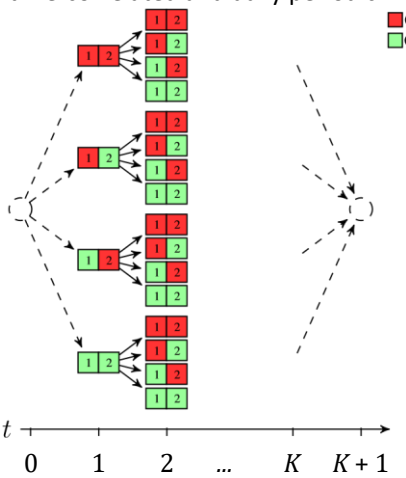

FIGURE 3. Graph showing the ON-OFF sequence possibilities in the case of a cluster with two SBSs in a HetNet scenario. Each node represents the state of the two SBSs (green color for the ON state and red color for the OFF state).
The two dashed nodes indicate the artificial nodes.

V. OPTIMAL LOAD CONTROL WITH ENERGY SHARING

In this section, we introduce the Load Control with Energy Sharing algorithm, which provides the optimal state selection of SBSs at every time instant, given the temporal evolution of the energy harvesting arrival and traffic load processes.

We represent the optimization problem in (3) as a graph. A node i at time t in the graph (V_i^t) represents a possible combination of states of the SBSs in the cluster. Each combination returns a different level of the batteries of the SBSs.

In Fig. 3 we report an example with a cluster of 2 SBSs in a HetNet scenario. In the first time step ($t = 1$) the SBSs can be in one of the four combinations of ON (green) / OFF (red) states. At each cycle t, the energy harvesting and traffic processes are evolving, based on H^t and L^t. Each node V_i^t generates 4 child nodes V_j^{t+1}, as possible combinations at the cycle $t + 1$. The battery levels of the child nodes V_j^{t+1} are calculated based on (1) and each arc connecting two nodes has a cost given by (4). The number of combinations is then evolving in time until reaching its maximum at time instant K. The cost associated with each arc, $f(\mathbf{S}_t,t)$, may be interpreted as the length of the corresponding arc. Two artificial nodes have been added at time step $t = 0$ and $t = K + 1$, to have a single initial node and a single terminal node. The cost associated with the arcs connecting the artificial nodes are set to zero. In this case, the problem of minimizing the total cost is equal to the problem of finding the path with the minimum-length from the initial to the terminal node. We tailor Label Correcting Algorithm [32] to efficiently explore the graph and find the shortest path. The algorithm steps are detailed in Algorithm 1. We define three variables: d^t_i, called label of V_i^t, as the length of the shortest path to the node V_i^t, OPEN as the list of nodes to be explored and UPPER as the last found minimum-length path to the terminal node. Moreover, N is the number of SBS in the cluster and γ is the number of states (i.e., $\gamma = 2$ for HetNets, and $\gamma = 3$ for MEC-H). The graph is explored in a depth-first fashion. The idea is to progressively discover shorter paths from the initial node to the internal nodes V_i^t till reaching the terminal node, and to maintain the length of the shortest path found so far in the variable d^t_i. Each time d^t_i is reduced following the discovery of a new shorter path to V_i^t, the algorithm checks to see if the labels d^{t+1}_j of the children V_j^{t+1} of V_i^t can be corrected, that is, they can be reduced by setting them to $d_i^t + A_{(i,t)}^{(j,t+1)}$, where $A_{(i,t)}^{(j,t+1)}$ is the arc(V_i^t, V_j^{t+1}). The list OPEN contains only the nodes that are candidates for further examination and possible inclusion in the shortest path. More specifically, we exclude from the list all those nodes that cannot satisfy the constraint on the battery and return a minimum path longer than UPPER.

Algorithm 1 Optimal loads control with energy sharing algorithm

initialize OPEN with possible states at time t while
OPEN is not empty do
remove a node V_i^t
compute battery value $B^{t+1}_j, j = 1,..,\gamma^N$, for all possible S^{t+1} using formula (1) for each node V_j^{t+1} child of V_i^t do
$A^{(+1)}_{(i,t)} = f(\boldsymbol{S}_j^{+1}, t+1)_{j,t}$ $_t$
if $d_i^t + A_{(i,t)}^{(j,t+1)} < \min\{d_j^{t+1}$,UPPER$\}$ and $B_j^{t+1} > B_{\text{th}}$ then
$d^{t+1}_j \leftarrow d_{ti} + A_{(j,t+1)}$
set parent of V_j^{t+1} V_i^t $^{(i,t)}$
if t 6= K then
place V_j^{t+1} in OPEN (if not already)
else
UPPER = $d_i^t + A_{(i,t)}^{(j,t+1)}$
end if
end if
end for
end while

VI. RESULTS AND DISCUSSION

We considered a square area with a side of 1 km and one MBS located in the center providing baseline coverage and computing resources. Three SBSs are positioned in hotspots for capacity enhancement. The coverage areas of the SBSs do not overlap. Energy arrivals and aggregated downlink traffic have been generated according to the realistic models described in Section IV.C. In particular, the city of Los Angeles has been used for generating the solar harvested energy traces. The adopted power consumption model is described in Section IV.B; parameter setup has been performed based on the values reported in [29]. The results provided in what follows are averaged among ten different independent realizations of both energy arrivals and traffic processes. In

TABLE 1. Simulation parameters

Parameter	Value
BS Bandwidth	5 MHz
Channel model	Okumura-Hata [33]
MBS TX power	43 dBm
SBS TX power	38 dBm
Solar modules	Panasonic N235B
Solar cell efficiency	21%
Traffic area	Residential
B_{th}	0.2
$w1,w2$	0.5

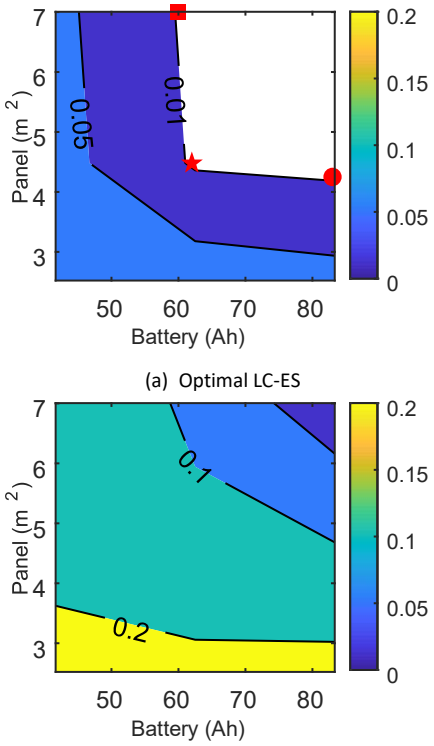

(a) Optimal LC-ES

(b) Naive

FIGURE 4. Contour plot of the traffic drop rate of LC-ES and the naive algorithm in a HetNet scenario. Different colors indicate traffic drop rate regions, whose maximum outage is specified in the color map in the right hand side of the plot. The white filled region indicates a traffic drop rate smaller than 1%.

the discussion presented next, we refer to January February, October, November and December as winter months; the remaining part of the year is considered as summer. Additional simulation parameters are listed in Table 1.

A. DIMENSIONING OF THE HARVESTING AND STORAGE SYSTEM

Fig. 4 and Fig. 5 show the contour plots of the traffic drop rate for HetNet and MEC-H, respectively, during the month of December (the worst in terms of harvested energy). Different colors are used to indicate traffic drop rate regions (maximum values are specified in the associated color map). The white

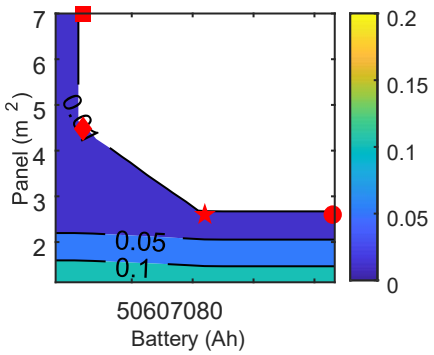

(a) Optimal LC-ES

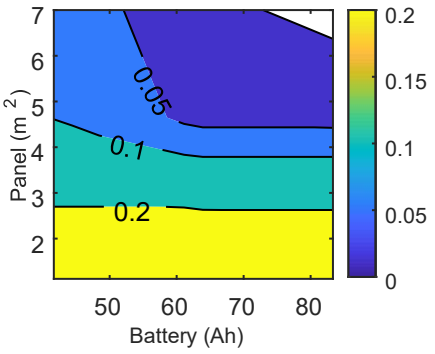

(b) Naive

FIGURE 5. Contour plot of the traffic drop rate of LC-ES and the naive algorithm in a MEC-H scenario. Different colors indicate traffic drop rate regions, whose maximum outage is specified in the color map in the right hand side of the plot. The white filled region indicates a traffic drop rate smaller than 1%.

filled area indicates the parameter region where the traffic drop is smaller than 1%. Our optimal analysis is compared with two naive approaches according to the network scenario. In HetNet architecture, the naive algorithm switches OFF a

SBS when its battery level is below a threshold and turns it ON when the battery is above. In MEC-H deployment, when the battery level is above the threshold the SBS is configured in the PHY-RF split mode, which is equivalent to the C-RAN operations, otherwise is in OFF state.

Taking 1% as our design parameter, all the points on the boundary of the white filled region are equally good. It is evident that the use of the optimal load control with energy sharing (LC-ES) allows the network to work with much lower sizes of the harvesting/storage system compared to the naive approaches. More in detail, MEC-H architecture presents lower harvesting/storage dimensions due to the higher number of SBS configuration options than HetNets deployments. These results confirm that an intelligent energy management system is essential for an efficient use of the renewable energy resource and its installation in town facilities.

The analysis in the following parts of the paper considers various harvesting/storage design approaches corresponding to the different points laying in the boundary of the white filled area of Fig. 4 and Fig. 5 and labeled with star, circle, square and diamond (in MEC-H deployment only).

B. SBSS OPERATIVE STATE CONFIGURATION

In Fig. 6 and Fig. 7, we report the different choices of the operative states of the SBSs by the optimal LC-ES across the different months of the year in HetNet and MEC-H, respectively. The graphs refer to the selected harvesting/storage dimensions.

In the HetNet scenario, SBSs are active and offload the MBS longer during the summer months (high energy

inflow). We can appreciate different behaviors based on the harvesting/storage dimensions: star approach ranges between 53% (in December) and 65% (in August) of time, circle between 56% (in December) and 76% (in July) of time and square between 59% (in December) and 64% (in July) of time.

Also in MEC-H scenario, SBSs offload the MBS for longer periods during the summer months, as expected. The length of the active periods and the choice of the operational mode depends on the specific harvesting/storage dimension. The SBS active period in the star deployment ranges between 54% (44% in PHY-RF mode and 10% in MAC-PHY, respectively, in December) and 78% (30% in PHY-RF mode and 48% in MAC-PHY, respectively, in August) of time; in the circle deployment between 55% (48% in PHY-RF and 9% in MAC-PHY, in December) and 80% (28% in PHY-RF, 52% in MAC-PHY, in August); in the diamond deployment between 65% (38% in PHY-RF, 27% in MAC-PHY, in December) and 73% (34% in PHY-RF, 39% in MAC-PHY, in August). Finally, the square deployment has an active period that ranges between 69% (39% in PHY-RF, 30% in MAC-PHY, in December) and 75% (32% in PHY-RF, 43% in MAC-PHY, in July) of the time.

PHY-RF split is the most chosen configuration option in the winter months, whereas MAC-PHY is the most prevalent in the summer months. A higher energy inflow allows the SBSs to locally perform their baseband processing, whereas in winter, the lower energy arrivals force the SBS to offload the baseband processing to the MBS and, hence, PHY-RF is the dominant operative mode. We observe that moving to the left side of the contour plot (i.e., bigger solar panels and smaller batteries) leads to longer activity during winter months and slightly shorter in summer.

We highlight here that MEC-H architecture allows longer active periods and offloading capabilities (i.e., MAC-PHY and PHY-RF operative modes) even with smaller dimensions of the harvesting/storage system than HetNet.

C. SHARED ENERGY ASSESSMENT

In Fig. 8 we show the energy shared and used by the MBS for every month of the year in both HetNet (8a) and MEC-H (8b) deployments. The graphs are collected considering the selected harvesting/storage design approaches. For comparison purposes, we also indicate the amount of shared energy using the naive approaches.

We observe a general trend of sharing a bigger amount of energy during the summer months, when a higher solar energy inflow occurs and, hence, a higher probability of exceeding the battery capacity of the SBSs. In HetNet, the square harvesting/storage deployment presents the highest amount of energy shared and the circle approach the poorest. Similar behavior is noticed in MEC-H, with the exception that the lowest performance is exhibited by the star design. The total amount of energy shared in HetNet scenario is normally higher than in MEC-H architecture, due to the bigger dimensions of the harvesting/solar system required to maintain the traffic demand.

VII. ENERGY SAVINGS AND COST ANALYSIS

In Table 2 we provide an energy and economic comparison between our LC-ES method and a scenario in which all the BSs are always active and supplied by the power grid. We refer to the latter as grid-connected. For the two architectural solutions, we report the grid energy consumption, the CAPital EXPenditures (CAPEX), the 1-year OPerational EXpenditures (OPEX) and the monetary cost (i.e., CAPEX + OPEX) due to the harvesting/storage add-on after 5 and 10 years, for the different panel and battery dimensions introduced in the previous section. The values between brackets indicate the savings with respect to the grid-connected scenario. We consider a cost of 1.17 $/W for the solar panel (which also includes the installation cost) and 131 $/kWh for the battery. Moreover, the energy purchased from the grid has a cost of 0.21 $/kWh in our calculation.

The additional harvesting/storage hardware jointly with the LC-ES method allows reducing the grid power consumption for both network deployments considered. The energy savings range between 22% and 30% for HetNet, and 16% and 48% for MEC-H, depending on the harvesting/storage size. Carbon footprint and OPEX are decreased accordingly. In particular, monetary cost savings range between 0.5% and 7% for HetNet, and 0.5% and 16% for MEC-H after 5 years. The only exception is represented by the third harvesting/storage size (i.e., square) in the HetNet scenario, where 7 years are needed to reach the breakeven point. The results at 10 years show higher savings, ranging between 11% and 18% for HetNet, and 8% and 32% for MEC-H.

Table 2 provides useful insights on the energy and cost savings and permits the MNOs to design their harvesting/storage systems by considering the tradeoff between dimensions and economic cost. In general, the harvesting/storage system with the lowest CAPEX is not the most economically convenient option in the long run. In HetNet, the highest savings are achieved for deployments in the right side of the boundary region of Fig. 4 (i.e., circle). With this design approach, LC-ES achieves the highest energy and cost savings by maintaining active the SBSs for longer periods and sharing less energy with the MBS compared to the other two harvesting/storage dimensions. In MEC-H, instead, the left side of Fig. 5 (i.e. square) is the most economically convenient option. Using these sizes, LC-ES is achieving higher savings by maintaining the SBSs operative for shorter periods in summer months and

sharing more energy with the MBS compared to the other harvesting/storage configurations.

As a final remark, we can assume that higher revenues and applied. In particular, a key identified challenge is to design intelligent energy management systems that may efficiently use the renewable energy inflow for autonomous operations via load control and energy sharing. The research

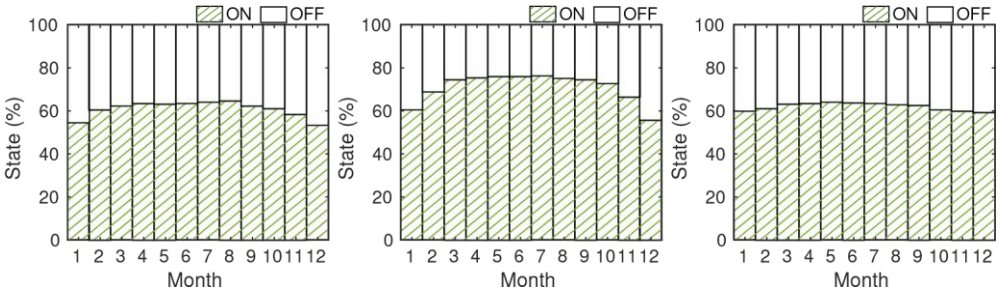

(a) 4.48 m² - 62 Ah [?] (b) 4.48 m² - 83 Ah [◦] (c) 7.00 m² - 62 Ah []

FIGURE 6. States selected by the LC-ES algorithm per month (in percentage) for different deployment sizes in the HetNet scenario.

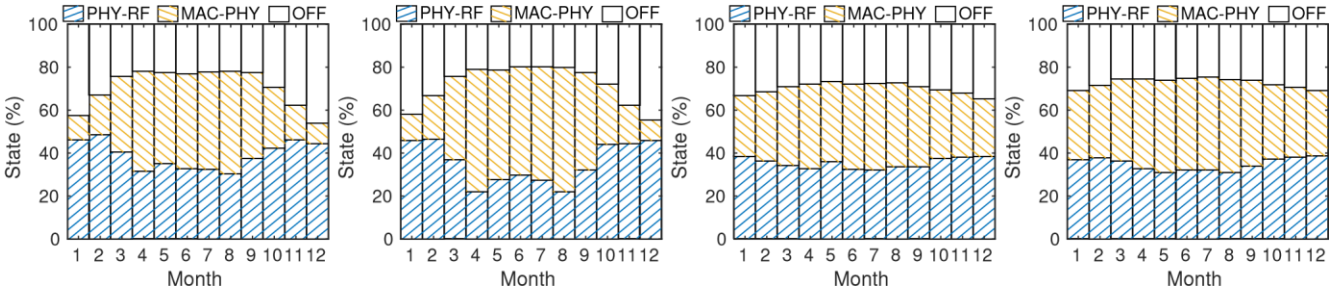

(a) 2.52 m² - 62 Ah [?] (b) 2.52 m² - 83 Ah [◦] (c) 4.48 m² - 42 Ah [◇] (d) 7.00 m² - 42 Ah []

FIGURE 7. States selected by the LC-ES algorithm per month (in percentage) for different deployment sizes in the MEC-H scenario.

TABLE 2. Energy savings and costs for different deployment dimensions

Architecture	Configuration		Energy (kW)	Costs ($)			
	panel (m²)	battery (Ah)	consumption [1yr]	CAPEX	OPEX [1yr]	cost [5yrs]	cost [10yrs]
Grid connected	-	-	10,264	0	2,155	10,775	21,550
HetNet	? 4.48	62	7,982 (-22%)	2,345	1,676	10,725 (-0.5%)	19,105 (-11%)
	◦ 4.48	83	7,160 (-30%)	2,541	1,503	10,060 (-7%)	17,578 (-18%)
	7.00	62	7,169 (-30%)	4,100	1,505	11,625 (+8%)	19,150 (-11%)
MEC-H	? 2.52	62	8,584 (-16%)	1,695	1,802	10,705 (-0.7%)	19,715 (-9%)
	◦ 2.52	83	8,515 (-17%)	1,891	1,788	10,831 (-0.5%)	19,771 (-8%)
	4.48	42	7,335 (-29%)	2,359	1,540	10,059 (-7%)	17,759 (-18%)
	7.00	42	5,373 (-48%)	3,464	1,128	9,104 (-16%)	14,744 (-32%)

savings can be achieved during the lifetime of the network in a near future considering that: i) equipment hardware is designed to be always more energy efficient, ii) the actual market trends show a decreasing cost of the solar panels and batteries, and increasing prices of the grid energy, iii) future radio access networks will be ultra-dense and longer offloading periods may occur due to the higher number of SBSs.

VIII. OPEN ISSUES AND FUTURE DIRECTIONS

Building on the above discussion, we believe that energy selfsufficiency of mobile networks is not far to be realized and is a fertile ground for research, both theoretical and activity in this new field is strongly encouraged by our results and represent a new frontier for green mobile networks. Therefore, a few fundamental problems are identified and discussed next.

A. CONTROL OF ULTRA-DENSE NETWORKS

It is expected that the next generation of mobile networks will be ultra-dense, which means having as many base stations as mobile users. Automatic and energy-aware configuration of such a high number of base stations is of enormous complexity, given the higher number of variables characterizing the system. The lack of spatio-temporal probabilistic models (e.g., channel interference, mobile

traffic, user mobility) is an open issue to be solved for a proper network optimization. Due to the complexity and the dynamism of this scenario, the definition of on-line control solution becomes crucial for designing algorithms able to reach the optimal performance. To this respect, reinforcement learning (RL) and the novel deep reinforcement learning (DRL) can be effective tools. In fact, these learning approaches are able to adapt to system dynamics without any a-priori knowledge by solving iteratively the control problem. A proper tradeoff between the accuracy and the complexity of the model is of paramount importance to find feasible and implementable solutions.

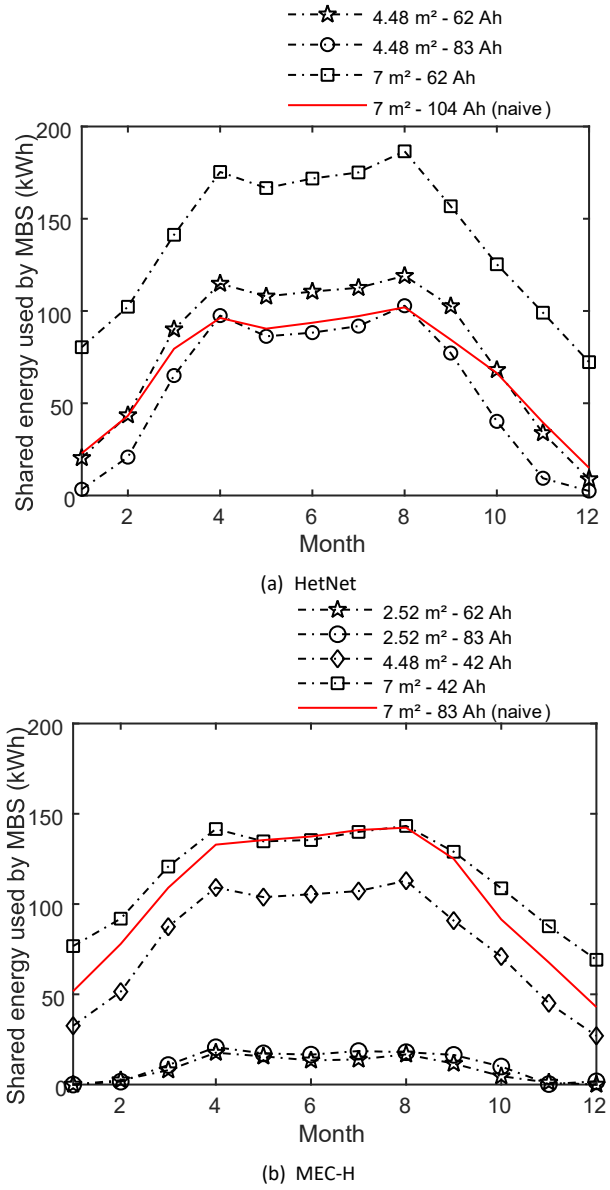

FIGURE 8. Energy shared by the SBSs and used by the MBS per month when considering different deployment sizes in (a) HetNet and (b) MEC-H architectures.

B. ENERGY SHARING AMONG THE SBSS

Sharing energy with the MBS may lead to high energy and cost savings, as discussed in the above. However, such cooperation method might be extended to assist also other SBSs that may, or may not, be supplied by additional harvesting/storage hardware. Moreover, exceeding energy may also provide ancillary services to other loads of the micro-grid. In this context, the Energy Packet Networks (EPNs) [17] represents a new architecture to be further explored for the energy transfer among micro-grid loads. In an EPN, discrete units of energy, termed energy packets, can be exchanged among the network elements. Energy routing protocols have to be designed to maintain the micro-grid stability and efficiently use the energy resource.

C. ENERGY TRADING AND INTEGRATION WITH THE SMART GRIDS

Trading is a solution for managing peaks of the energy demand in the smart grids [34] and includes the possibility of buying / selling the generated energy from / to other retailers. As introduced in [10], this solution will be interesting when proper pricing schemes will be in place. They should incentivize BSs to sell their excess energy, while, at the same time, making these transactions convenient for the power grid operators. In the next future, the energy price will depend on the cost of production and on the expected demand. In this scenario, future work shall evaluate decisionmaking solutions to find the best energy-purchasing policies for the BSs taking into account: (i) the current and forecast renewable energy inflow, (ii) the current and forecast traffic load, and (iii) the future evolution of the energy prices. In this scenario, BSs will act as prosumers of the smart grids.

IX. CONCLUSIONS

This paper has presented an optimal traffic and computational load control method with energy sharing to efficiently use the renewable energy coming from distributed sources and to facilitate the off-grid operation of the radio access network. Two architectures have been targeted: HetNet and MEC-H. The proposed approach enables the dynamic switch ON/OFF of portions of the SBSs in HetNets and permits to move and execute some of the transmission functions of the SBSs at the MBS site in MEC-H. Energy exceeding the battery capacity is managed to be used by the MBS operations and further reduce the energy drained from the power grid. Software simulations demonstrate that an intelligent renewable energy management is essential to reduce the harvesting/storage dimensions with respect to naive approaches and leads to high energy and cost savings for a Mobile Network Operator. Finally, open issues, research directions and

possible methodological approaches are discussed to encourage further studies in this area.

REFERENCES

[1] ETSI, "ES 203 208; Environmental Engineering (EE); Assessment of mobile network energy efficiency (v1.2.1)," 2017.
[2] 3GPP, "TR 21.866.; ; E-U; Study on Energy Efficiency Aspects of 3GPP Standards v15," 2017.
[3] W. V. Heddeghem, S. Lambert, B. Lannoo, D. Colle, M. Pickavet, and P. Demeester, "Trends in worldwide ict electricity consumption from 2007 to 2012," Computer Communications, vol. 50, pp. 64 – 76, 2014.
[4] A. S. Andrae and T. Edler, "On global electricity usage of communication technology: trends to 2030," MDPI Challenges, vol. 6, no. 1, pp. 117–157, April 2015.
[5] F. Han, S. Zhao, L. Zhang, and J. Wu, "Survey of Strategies for Switching Off Base Stations in Heterogeneous Networks for Greener 5G Systems," IEEE Access, vol. 4, pp. 4959–4973, August 2016.
[6] Y. Kabalci, "A survey on smart metering and smart grid communication," Renewable and Sustainable Energy Reviews, vol. 57, pp. 302 – 318, 2016.
[7] D. T. Ton and M. A. Smith, "The u.s. department of energy's microgrid initiative," The Electricity Journal, vol. 25, no. 8, pp. 84 – 94, 2012.
[8] H. A. H. Hassan, L. Nuaymi, and A. Pelov, "Renewable energy in cellular networks: A survey," in 2013 IEEE Online Conference on Green Communications (OnlineGreenComm), October 2013, pp. 1–7.
[9] G. Piro, M. Miozzo, G. Forte, N. Baldo, L. A. Grieco, G. Boggia, and P. Dini, "HetNets Powered by Renewable Energy Sources: Sustainable Next-Generation Cellular Networks," IEEE Internet Computing, vol. 17, no. 1, pp. 32–39, January 2013.
[10] D. Zordan, M. Miozzo, P. Dini, and M. Rossi, "When telecommunications networks meet energy grids: Cellular networks with energy harvesting and trading capabilities," IEEE Communications Magazine, vol. 53, no. 6, pp. 117–123, June 2015.
[11] D. López-Pérez, M. Ding, H. Claussen, and A. H. Jafari, "Towards 1 Gbps/UE in cellular systems: Understanding ultra-dense small cell deployments," IEEE Communications Surveys & Tutorials, vol. 17, no. 4, pp. 2078–2101, June 2015.
[12] N. Abbas, Y. Zhang, A. Taherkordi, and T. Skeie, "Mobile edge computing: A survey," IEEE Internet of Things Journal, vol. 5, no. 1, pp. 450–465, February 2018.
[13] A. G. Tsikalakis and N. D. Hatziargyriou, "Centralized control for optimizing microgrids operation," in 2011 IEEE Power and Energy Society General Meeting, July 2011, pp. 1–8.
[14] C. Park and J. Lee, "Mobile edge computing-enabled heterogeneous networks," CoRR, vol. abs/1804.07756, 2018. [Online]. Available: http://arxiv.org/abs/1804.07756
[15] J. Xu, L. Duan, and R. Zhang, "Cost-aware green cellular networks with energy and communication cooperation," IEEE Communications Magazine, vol. 53, no. 5, pp. 257–263, May 2015.
[16] J. Xu and R. Zhang, "CoMP Meets Smart Grid: A New Communication and Energy Cooperation Paradigm," IEEE Transactions on Vehicular Technology, vol. 64, no. 6, pp. 2476–2488, June 2015.
[17] E. Gelenbe and E. T. Ceran, "Energy Packet Networks With Energy Harvesting," IEEE Access, vol. 4, pp. 1321–1331, March 2016.
[18] B. Kreiner and J. Reeves, "Packetized power," January 2014, US Patent App. 14/010,674. [Online]. Available: http://google.com/patents/US20140013146
[19] B. Gurakan, O. Ozel, J. Yang, and S. Ulukus, "Energy cooperation in energy harvesting communications," IEEE Transactions on Communications, vol. 61, no. 12, pp. 4884–4898, December 2013.
[20] G. Zheng, Z. Ho, E. A. Jorswieck, and B. Ottersten, "Information and energy cooperation in cognitive radio networks," IEEE Transactions on Signal Processing, vol. 62, no. 9, pp. 2290–2303, May 2014.
[21] C. R. Valenta and G. D. Durgin, "Harvesting wireless power: Survey of energy-harvester conversion efficiency in far-field, wireless power transfer systems," IEEE Microwave Magazine, vol. 15, no. 4, pp. 108–120, June 2014.
[22] L. Bonati, A. F. Gambin, and M. Rossi, "Wireless power transfer under the spotlight: Charging terminals amid dense cellular networks," in IEEE International Symposium on A World of Wireless, Mobile and Multimedia Networks (WoWMoM), Macau, China, June 2017, pp. 1–9.
[23] NEC, "NFV C-RAN for Efficient RAN Resource Allocation," http://www.nec.com/en/global/solutions/nsp/sc2/doc/wp_c-ran.pdf, online White Paper; accessed on March 16, 2016.
[24] A. Lara, A. Kolasani, and B. Ramamurthy, "Network innovation using openflow: A survey," IEEE Communications Surveys Tutorials, vol. 16, no. 1, pp. 493–512, First 2014.
[25] 3GPP, "TS 38.801.; ; E-U; Study on new radio access technology: Radio access architecture and interfaces v14," 2017.
[26] B. Lindemark and G. Oberg, "Solar power for radio base station (rbs) sites applications including system dimensioning, cell planning and operation," in Twenty-Third International Telecommunications Energy Conference INTELEC 2001, October 2001, pp. 587–590.
[27] L. Lu, X. Han, J. Li, J. Hua, and M. Ouyang, "A review on the key issues for lithium-ion battery management in electric vehicles," Journal of Power Sources, vol. 226, pp. 272–288, 2013.
[28] "Virtualization for small cells: overview," Small cell forum, 2015.
[29] C. Desset, B. Debaillie, V. Giannini, A. Fehske, G. Auer, H. Holtkamp, W. Wajda, D. Sabella, F. Richter, M. J. Gonzalez et al., "Flexible power modeling of lte base stations," in IEEE Wireless Communications and Networking Conference (WCNC), Paris, France, April 2012, pp. 2858–2862.
[30] M. Miozzo, D. Zordan, P. Dini, and M. Rossi, "SolarStat: Modeling photovoltaic sources through stochastic Markov processes," in IEEE International Energy Conference (ENERGYCON), Cavtat, Croatia, May 2014, pp. 688–695.
[31] F. Xu, Y. Li, H. Wang, P. Zhang, and D. Jin, "Understanding Mobile Traffic Patterns of Large Scale Cellular Towers in Urban Environment," IEEE/ACM Trans. Netw., vol. 25, no. 2, pp. 1147–1161, April 2017.
[32] D. P. Bertsekas, Dynamic programming and optimal control. Athena scientific Belmont, MA, 1995, vol. 1, no. 2.
[33] M. Hata, "Empirical formula for propagation loss in land mobile radio services," IEEE Transactions on Vehicular Technology, vol. 29, no. 3, pp. 317–325, August 1980.
[34] I. S. Bayram, M. Z. Shakir, M. Abdallah, and K. Qaraqe, "A survey on energy trading in smart grid," in IEEE Global Conference on Signal and Information Processing (GlobalSIP), Atlanta, GA, USA, December 2014, pp. 258–262